

Gamow-Teller transition strengths in the intermediate nucleus of the ^{116}Cd double- β decay by the $^{116}\text{Cd}(p,n)^{116}\text{In}$ and $^{116}\text{Sn}(n,p)^{116}\text{In}$ reactions at 300 MeV

M. Sasano,^{1,*} H. Sakai,¹ K. Yako,¹ T. Wakasa,² M. Dozono,² V. Rodin,³ A. Faessler,³ K. Fujita,² M. B. Greenfield,⁴ K. Hatanaka,⁵ K. Itoh,⁶ T. Kawabata,⁷ H. Kuboki,¹ Y. Maeda,⁸ K. Miki,¹ K. Muto,⁹ S. Noji,¹ H. Okamura,⁵ Y. Sakemi,¹⁰ K. Sekiguchi,¹¹ Y. Shimizu,⁷ Y. Sasamoto,⁷ Y. Tameshige,⁵ A. Tamii,⁵ and T. Uesaka⁷

¹Department of Physics, The University of Tokyo, Bunkyo, Tokyo 113-0033, Japan

²Department of Physics, Kyushu University, Higashi, Fukuoka 812-8581, Japan

³Institut für Theoretische Physik, Universität Tübingen, Tübingen D-72076, Germany

⁴Department of Physics, International Christian University, Mitaka, Tokyo 181-8585, Japan

⁵Research Center for Nuclear Physics (RCNP), Osaka University, Ibaraki, Osaka 567-0047, Japan

⁶Department of Physics, Saitama University, Saitama 338-8570, Japan

⁷Center for Nuclear Study, The University of Tokyo, Bunkyo, Tokyo 113-0033, Japan

⁸Department of Applied Physics, University of Miyazaki, Kibanadai-nishi, Miyazaki-shi 889-2192, Japan

⁹Department of Physics, Tokyo Institute of Technology, Meguro, Tokyo 152-8550, Japan

¹⁰Cyclotron and Radioisotope Center, Tohoku University, Aoba-ku, Sendai 980-8578, Japan

¹¹RIKEN Nishina Center, Wako, Saitama 351-0198, Japan

(Received 15 April 2012; published 6 June 2012)

The double-differential cross sections for the $^{116}\text{Cd}(p,n)$ and $^{116}\text{Sn}(n,p)$ reactions were measured at 300 MeV for studying the nuclear matrix element of the ^{116}Cd $\beta\beta$ decay. A multipole decomposition technique was applied to the spectra to extract the Gamow-Teller (GT) component. The integrated GT strengths up to an excitation energy of 30 MeV in the intermediate nucleus ^{116}In are 40 ± 6 and 11 ± 1 in the (p,n) and (n,p) spectra, respectively, including the component from the isovector spin monopole (IVSM). The spectra are compared with those obtained from a theoretical calculation with a quasiparticle random phase approximation, where the contribution from the IVSM component as well as the interference effect between the GT and IVSM components are fully taken into account.

DOI: 10.1103/PhysRevC.85.061301

PACS number(s): 25.40.Kv, 23.40.-s, 24.30.Gd, 27.60.+j

The two modes of double- β ($\beta\beta$) decay, two-neutrino ($2\nu\beta\beta$) [1] and neutrinoless ($0\nu\beta\beta$) [2], have received a great deal of interest in the nuclear and particle physics communities. A half-life of the $0\nu\beta\beta$ mode, if measured with large-scale direct counting experiments [3], would constrain the absolute scale of neutrino masses [4]. An indispensable factor for interpreting a measured half-life is the nuclear matrix element $M^{0\nu}$, which depends on details of nuclear structures and is only theoretically evaluated by using nuclear-model calculations. On the other hand, the $2\nu\beta\beta$ mode is a second-order allowed weak process. Its nuclear matrix element $M^{2\nu}$ is directly derived from the half-lives measured on several nuclei [5]. As the $2\nu\beta\beta$ mode connects the same initial and final nuclear ground states as the $0\nu\beta\beta$ mode, the understanding of the nuclear structures embedded in $M^{2\nu}$ is an important step toward a reliable estimate of $M^{0\nu}$.

The $M^{2\nu}$ from the initial ground 0^+ state $|0_{\text{g.s.}}^i\rangle$ to the final ground 0^+ state $|0_{\text{g.s.}}^f\rangle$ is given by [4]

$$M^{2\nu} = \sum_m \frac{\langle 0_{\text{g.s.}}^f | O_{\text{GT}^-} | 1_m^+ \rangle \langle 1_m^+ | O_{\text{GT}^-} | 0_{\text{g.s.}}^i \rangle}{E_{x,m} + M - (M_i + M_f)/2}. \quad (1)$$

Here the summation is over all 1^+ states in the intermediate nucleus. We note that, in the case of $M^{0\nu}$, the intermediate

state runs over all J^π values. The excitation energy of the m th 1^+ state $|1_m^+\rangle$ in the intermediate nucleus is denoted as $E_{x,m}$. The term $M - (M_i + M_f)/2$ is the difference of the mass of the intermediate nucleus (M) from the averaged mass of the initial (M_i) and final (M_f) nuclei. The symbol O_{GT^-} indicates the operator for the Gamow-Teller (GT) transition in the β^- direction defined as $O_{\text{GT}^-} = \sum_k \sigma_k t_{-k}$. Here the subscript k runs over all the neutrons of the decaying nucleus. This operator involves spin and isospin transfers ($\Delta S = \Delta T = 1$) without changing the angular momentum ($\Delta L = 0$) in the same major shell ($0\hbar\omega$). The numerator is the contribution from the m th 1^+ intermediate state to $M^{2\nu}$, which is the product of the GT matrix elements from the initial state to the intermediate state and from the intermediate state to the final state. The contributions from the 1^+ intermediate states to $M^{2\nu}$ are correlated with the corresponding part in $M^{0\nu}$, which connects the same initial and final states through the 1^+ intermediate states (see Fig. 8 in Ref. [6]). Thus, the studies of the $M^{2\nu}$ will lead to a more reliable estimate of $M^{0\nu}$, though the important contributions to $M^{0\nu}$ come from intermediate states with several J^π values.

An experimental approach is the study of the GT strength [$B(\text{GT}^\pm)$] distributions, where Eq. (1) is replaced with a running sum

$$M_+^{2\nu}(E) = \sum_m^{E_{x,m} < E} \frac{\sqrt{B(\text{GT}^-; m)} \sqrt{B(\text{GT}^+; m)}}{E_{x,m} + Q_{\text{EC}} + Q_{\beta\beta}/2}. \quad (2)$$

*Present address: RIKEN Nishina Center, Wako, Saitama 351-0198, Japan.

Here the contributions from different intermediate states are added constructively, i.e., neglecting the phase of the GT matrix elements, because there is no experimental means to determine the phase. The parameter E represents the excitation-energy upper limit of the summation. Values of $B(\text{GT}^-)$ and $B(\text{GT}^+)$ can be determined by measuring the charge-exchange (CE) reactions of the (p,n) and (n,p) types on the initial and final nuclei, respectively. The $\Delta L = 0$ cross section at 0° , $\sigma_{\Delta L=0}(0^\circ)$, can be converted to $B(\text{GT})$ by using the well-established proportionality relation

$$\sigma_{\Delta L=0}(0^\circ) = \hat{\sigma}_{\text{GT}} F(q, \omega) B(\text{GT}), \quad (3)$$

where $\hat{\sigma}_{\text{GT}}$ is the GT unit cross section and $F(q, \omega)$ is the kinematic correction factor [7].

Recently, Yako *et al.* have studied the $B(\text{GT}^\pm)$ distributions in the intermediate nucleus ^{48}Sc of the ^{48}Ca $\beta\beta$ decay via the $^{48}\text{Ca}(p,n)$ and $^{48}\text{Ti}(n,p)$ reactions at 300 MeV [8]. Therein, unexpectedly large strengths were found in the continuum above 8 MeV of the (n,p) spectra, where almost no GT strength is predicted with a shell-model calculation within the full fp shell-model space. This discrepancy suggests that the present shell-model description of $M^{2\nu}$ may need to be refined. It is compelling to know whether such high-lying intermediate states exist in heavier $\beta\beta$ -decay nuclei, because all the $\beta\beta$ -decay nuclei studied by the large-scale experiments lie in the mass region of $A \geq 76$, except for ^{48}Ca .

The ^{116}Cd $0\nu\beta\beta$ decay has been intensively studied by several groups [9]. These studies also lead to the half-life of the $2\nu\beta\beta$ decay, $(3.0 \pm 0.2) \times 10^{19}$ y [5], from which the $M^{2\nu}$ value is derived as 0.127 MeV^{-1} with an accuracy of 3% by following the method in Ref. [10]. Nevertheless, the situation regarding studies of $B(\text{GT}^\pm)$ [11–15] is rather unsatisfactory; low-lying GT states in ^{116}In up to 3 MeV were successfully identified by the high-resolution measurement of the $^{116}\text{Sn}(d,^2\text{He})$ reaction [15], and were combined with the data by the $^{116}\text{Cd}(^3\text{He},t)$ reaction [12]. Recently, however, the $B(\text{GT}^-)$ data reported in Ref. [12] have been found to be incorrect, because, in the experiment, a Cd target with natural isotopic abundance was improperly used instead of a ^{116}Cd target.

In this Rapid Communication, the $B(\text{GT}^-)$ and $B(\text{GT}^+)$ distributions in ^{116}In are derived for a wide excitation energy region up to 30 MeV by the $^{116}\text{Cd}(p,n)$ and $^{116}\text{Sn}(n,p)$ reactions at 300 MeV, respectively. At 300 MeV, the spin-flip cross sections are large and distortion effects are minimal [16] so that the characteristic shapes of the angular distributions for each angular momentum transfer are very distinct. These favorable features allow us to extract the $B(\text{GT}^\pm)$ distributions in the continuum by multipole decomposition (MD) analysis [17]. The MD analysis of the (n,p) spectra is less reliable at higher energies, while that of the (p,n) spectra is stable up to 40 MeV.

The extraction of $B(\text{GT}^+)$ in the continuum is often hampered by the existence of an isovector spin monopole resonance (IVSM) [8]. This mode is a $2\hbar\omega$ excitation via the $r^2\sigma t_\pm$ operator, being mixed with the GT excitation by the residual interaction because it has the same $J^\pi = 1^+$ [18]. This mixing can affect the CE cross sections through

the interference effect between the GT and IVSM scattering amplitudes. Nevertheless, in Ref. [8], the IVSM contribution is estimated rather simply by assuming IVSM to be a normal mode excitation [19]. Herein, we employ a new approach based on a microscopic method [20] to compare our experimental spectra directly with the calculated ones, which take into account the IVSM components as well as their interference with the GT components.

Both (p,n) and (n,p) experiments were carried out at the Research Center for Nuclear Physics (RCNP) of Osaka University, by using 295-MeV proton beams. The (p,n) data were obtained by using the neutron time-of-flight (NTOF) facility [21] in conjunction with the neutron detection system NPOL3 [22]. A self-supporting metallic foil isotopically enriched to ^{116}Cd ($>99.5\%$) with a thickness of $103 \pm 5 \text{ mg/cm}^2$ was used. The scattering angle varied from 0° to 14° in step of 2° in the laboratory frame. The (n,p) data were taken with the (n,p) facility [23]. A neutron beam at 293 MeV with an intensity of $1 \times 10^6 \text{ s}^{-1}$ was produced by using a proton beam with a current of 300 nA through the $^7\text{Li}(p,n)$ reaction and, then, incident on the three enriched ^{116}Sn (99.6%) target foils with thicknesses of 310 ± 12 , 338 ± 13 , and $419 \pm 16 \text{ mg/cm}^2$ mounted in a multitarget system. The spectra obtained over an angular range of 0° – 12° were divided into 12 spectra of double-differential cross sections in 1° bins. The overall energy resolutions were about 500 keV and 2.2 MeV in the (p,n) and (n,p) spectra, respectively.

The dots in Fig. 1 show the spectra for the $^{116}\text{Cd}(p,n)$ and $^{116}\text{Sn}(n,p)$ reactions near 0° , 4° , and 10° as a function of the excitation energy in ^{116}In . The vertical bars indicate the statistical uncertainties, which are typically 2% per each energy bin with the widths of 0.5 and 1.0 MeV in the (p,n) and (n,p) spectra, respectively. The hatched areas in Fig. 1 show the result of the MD analysis, where the cross sections are decomposed into multipole components from

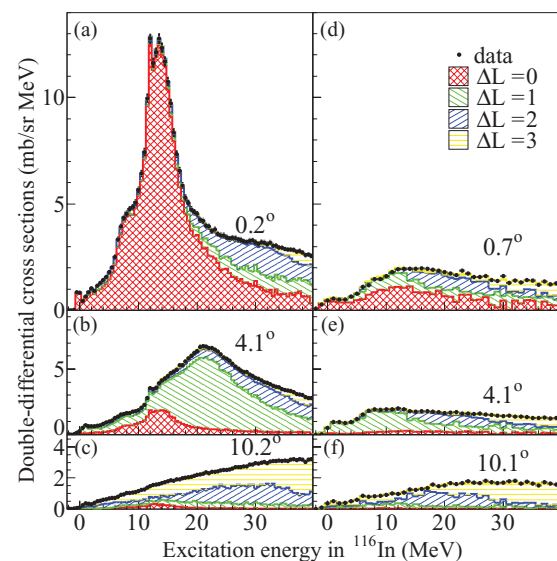


FIG. 1. (Color) Double-differential cross sections and the MD-analysis results for the $^{116}\text{Cd}(p,n)$ (a)–(c) and for the $^{116}\text{Sn}(n,p)$ (d)–(f) reactions near 0° (a), (d), 4° (b), (e), and 10° (c), (f).

$\Delta L = 0$ to 3 as described in Ref. [8]. In the MD analysis, the experimental angular distribution of the cross section included in each energy bin was fitted by using a linear combination of angular distributions calculated with a distorted wave impulse approximation (DWIA). Here the computer code DW81 [24] was used with the input parameters of the effective interactions at 325 MeV by Franey and Love [25] and the optical potential by Cooper and Hama [26] (without the Coulomb interaction for neutrons). The MD analysis of the (n, p) spectra becomes unstable above about 30-MeV excitation. Thus, we will focus on the intermediate states below 30 MeV.

The dots in Figs. 2(a) and 2(b) show the strength distributions derived from the $\Delta L = 0$ cross section through Eq. (3). Here the $\hat{\sigma}_{GT}$ value was estimated to be 3.0 ± 0.3 mb/sr from the nuclear mass number (A) dependence of $\hat{\sigma}_{GT}$ taken from Ref. [27]. The vertical bars indicate the statistical uncertainties. The strength is denoted as $B(GT + IVSM)$ because it contains the IVSM component. The GT plus IVSM strengths integrated up to an excitation energy of 30 MeV of ^{116}In are $\sum B(GT^- + IVSM^-) = 40 \pm 6$ and $B(GT^+ + IVSM^+) = 11 \pm 1$, where the uncertainties are the quadratic sums of the statistical uncertainties (2% and 5%), the systematic uncertainties in the cross sections (5% and 6%),

MD analysis (13% and 3%), $F(q, \omega)$ (2% and 1%), and the $\hat{\sigma}_{GT}$ value (10%), respectively.

In the β^- direction, the GT strength for the transition from the ^{116}Cd ground state to the ^{116}In ground state, $B[GT^-; ^{116}\text{In}(\text{g.s.})]$, is deduced to be 0.28 ± 0.03 from the corresponding 0° cross section of 0.83 ± 0.06 mb/sr already published in Ref. [28]. The present $B[GT^-; ^{116}\text{In}(\text{g.s.})]$ value is almost consistent with the value of 0.47 ± 0.13 by the electron-capture (EC) experiment [13]. However, the values of 0.16 ± 0.02 and 0.14 ± 0.03 reported in the study of the low-energy (p, n) reaction at 35 MeV [11] and in the Erratum of the $(^3\text{He}, t)$ study [12] are significantly smaller than the present value by 30%.

In the β^+ direction, the individual low-lying states observed in the high-resolution $(d, ^2\text{He})$ experiment [15] are not separated herein because of a rather limited energy resolution of the (n, p) spectra. The shaded area in Fig. 2(b) shows the spectrum for the $B(GT^+)$ values by the $(d, ^2\text{He})$ study smeared with our energy resolution of 2.2 MeV. The present spectrum well agrees with the $(d, ^2\text{He})$ result, but clearly shows the existence of additional strengths above 3 MeV.

The contribution from the IVSM component is evaluated by employing a microscopic method of Ref. [20], where DWIA calculations are performed with realistic transition densities calculated within the framework of a quasiparticle random phase approximation (QRPA). A large model space ($8\hbar\omega$, 34 single-particle states) is chosen for describing both the GT and IVSM excitations. The QRPA model parameters are fixed in the same manner as done in Ref. [29] for the M^{0v} prediction. The renormalization factor $g_{pp} = 0.50$ for the particle-particle part of the residual interaction (the Brueckner G-matrix for CD Bonn NN force) and the quenching factor of 0.6744 for the GT transition densities are adjusted to reproduce the $2\nu\beta\beta$ -decay rate [5] and the EC and β -decay rates from the ^{116}In ground state [13,14]. Here the IVSM transition densities are not quenched because there is currently no experimental information on the quenching of IVSM. The spin-quadrupole ($J^\pi = 1^+$, $\Delta L = 2$) contributions are subtracted from all the transition densities.

The calculated cross sections are converted to strengths through Eq. (3) as the experimental cross sections are processed. Thus obtained strengths are shown with solid curves in Figs. 2(a) and 2(b), including both GT and IVSM components as well as the interference effect between them. The dashed and dotted curves are obtained separately from the GT and IVSM transition densities. The difference of the solid curve from the incoherent sum of the strengths shown by the dashed and dotted curves corresponds to the interference effect between GT and IVSM scattering amplitudes. All the curves are smeared by a Gaussian shape with an energy-dependent escape width $\Gamma^\downarrow(E)$ taken from the parametrization of Ref. [30] plus the experimental energy resolution.

The calculated $B(GT^- + IVSM^-)$ distribution is dominated by the GT component up to 20 MeV, including the GT giant resonance (GTGR). Above this energy, there is no significant amount of GT strength in the calculation. A bump of the IVSM resonance is predicted to lie around 32 MeV. The interference effect between the GT and IVSM components is about 10% of the GT plus IVSM strength, changing from constructive to

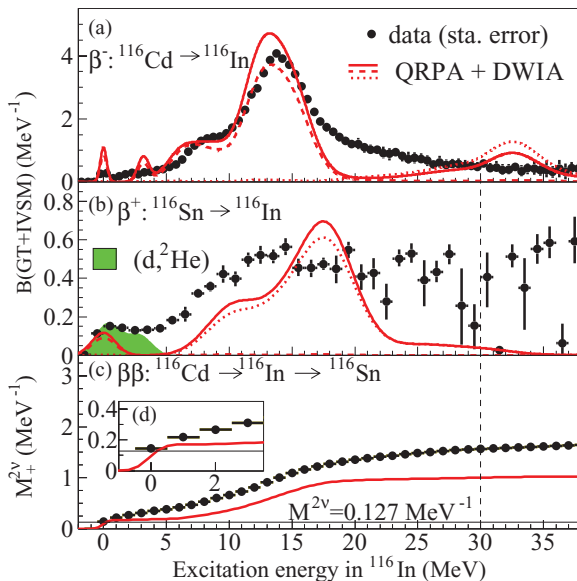


FIG. 2. (Color) Extracted GT strength distributions (dots) for the transitions connecting the initial ^{116}Cd (a) and final ^{116}Sn (b) ground states with the intermediate states of ^{116}In , including the IVSM component. The shaded area in (b) represents the $B(GT^+)$ distribution by the $(d, ^2\text{He})$ experiment [15]. The curves are the results derived through the DWIA calculations from the QRPA transition densities corresponding to GT plus IVSM (solid), GT (dashed), IVSM (dotted) excitations. (c) Values of $M^{2\nu}$ obtained from the experimental (dots) and theoretical (solid curve) GT plus IVSM strengths. The thin horizontal line shows the $M^{2\nu}$ value by the decay measurement [5]. The vertical dashed line in (b) and (c) is the upper limit of the MD analysis, above which the MD analysis for the (n, p) spectra is unstable. (d) shows the magnification of (c) in the energy region up to 3 MeV.

destructive around 18 MeV. On the other hand, the calculated GT^+ plus $IVSM^+$ strengths are mostly due to the IVSM resonance over a whole excitation energy region. A significant amount of GT strength exists only for the ground state. The interference effect is constructive, being independent of the excitation energy. In the energy region of the IVSM resonance, the tendency of the interference effect to be destructive and constructive in the β^- and β^+ directions, respectively, seems to agree with that predicted in Ref. [18].

The calculated GT^- plus $IVSM^-$ strengths qualitatively agree with the experimental ones below 15 MeV. Although the calculated spectrum has a prominent peak of IVSM around 32 MeV, there is no signature of the existence of IVSM in the experimental spectrum. However, this may be understood if the IVSM component is more spread than in the present calculation. In contrast, the agreement between the calculated and experimental $B(GT^+ + IVSM^+)$ distributions is rather poor; half of the strength up to 30 MeV identified herein can be explained by this calculation. We note the discrepancy becomes larger if the calculated IVSM component is quenched.

The dots in Fig. 2(c) show the $M_+^{2\nu}$ values obtained through Eq. (2) from the experimental $B(GT^\pm + IVSM^\pm)$ distributions. The $M_+^{2\nu}$ rapidly increases as a function of the excitation energy up to about 20 MeV, indicating the energy denominator in Eq. (2) does not diminish the importance of the strengths in this energy region. In the energy region where almost no IVSM component is predicted, the $M_+^{2\nu}$ value varies from $M_+^{2\nu} = 0.14 \pm 0.01 \text{ MeV}^{-1}$ at 0 MeV to $0.31 \pm 0.01 \text{ MeV}^{-1}$ at 3 MeV, as shown in Fig. 2(d). Here the $M_+^{2\nu}$ value at 0 MeV is derived from the present $B[GT^-, ^{116}\text{In}(g.s.)]$ value and the corresponding $B[GT^+, ^{116}\text{In}(g.s.)]$ value of 0.256 ± 0.001 by the β -decay measurement [14]. The large deviation of $M_+^{2\nu}$ from the $M^{2\nu}$ value indicates a possible cancellation effect between different intermediate states due to their phase differences neglected in the definition of $M_+^{2\nu}$.

Above 3 MeV, we compare the experimental $M_+^{2\nu}$ values with the theoretical $M_+^{2\nu}$ curve obtained from the calculated $B(GT^\pm + IVSM^\pm)$ distributions through Eq. (2), because the present strengths include the contribution from the IVSM component. The difference between the experimental and theoretical $M_+^{2\nu}$ values is 0.5 MeV^{-1} at 30 MeV. Thus, the present description of $M^{2\nu}$ does not fully take into account the intermediate 1^+ states involved in $M^{2\nu}$ or the MD analysis at higher energies is less reliable.

In summary, we obtained the GT strengths for the transitions to the intermediate 1^+ states up to 30 MeV in ^{116}In , in the β^- and β^+ directions via the $^{116}\text{Cd}(p,n)$ and $^{116}\text{Sn}(n,p)$ reactions at 300 MeV. The strengths integrated up to 30 MeV including the IVSM component are 40 ± 6 and 11 ± 1 in the β^- and β^+ directions, respectively. The GT strength from the ^{116}Cd ground state to the ^{116}In ground state is deduced to be 0.28 ± 0.03 . The experimental spectra were compared directly with the calculated ones based on the QRPA prediction used for the $M^{0\nu}$ prediction, taking into account the IVSM components as well as their interference effect with the GT components. The present spectrum in the β^- direction is qualitatively reproduced by the calculation except for the region above the GTGR. Half of the measured strength up to 30 MeV in the β^+ direction is reproduced by the calculation. The present nuclear-model calculation used for $M^{0\nu}$ prediction can be improved by including further correlations to reproduce the strength distributions and the $M^{2\nu}$ value consistently.

We are grateful to the accelerator group of RCNP for their efforts in providing a high-quality proton beam, which is indispensable for a good energy resolution. The experiments were performed at RCNP, Osaka University under the Experimental Programs No. E272 and No. E290. This work was supported financially in part by a Grant-in-Aid for Specially Promoted Research No. 17002003 of the Ministry of Education, Culture, Sports, Science, and Technology of Japan.

-
- [1] M. Goeppert-Mayer, *Phys. Rev.* **48**, 512 (1935).
 [2] W. Furry, *Phys. Rev.* **56**, 1184 (1939).
 [3] F. T. Avignone, S. R. Elliot, and J. Engel, *Rev. Mod. Phys.* **80**, 481 (2008).
 [4] S. R. Elliott and P. Vogel, *Annu. Rev. Nucl. Part. Sci.* **52**, 115 (2002); J. Suhonen and O. Civitarese, *Phys. Rep.* **300**, 123 (1998); A. Faessler and F. Šimkovic, *J. Phys. G* **24**, 2139 (1998).
 [5] A. S. Barabash, *Czech. J. Phys.* **56**, 1572 (2006).
 [6] V. A. Rodin, Amand Faessler, F. Šimkovic, and Petr Vogel, *Nucl. Phys. A* **766**, 107 (2006).
 [7] T. N. Taddeucci *et al.*, *Nucl. Phys. A* **469**, 125 (1987).
 [8] K. Yako *et al.*, *Phys. Rev. Lett.* **103**, 012503 (2009).
 [9] D. Y. Stewart *et al.* (COBRA Collaboration), *Nucl. Instrum. Methods Phys. Res. Sect. A* **580**, 342 (2007); Z. Daraktchieva *et al.* (NEMO Collaboration), *Nucl. Phys. A* **827**, 495c (2009).
 [10] F. Boehm and P. Vogel, *Annu. Rev. Nucl. Part. Sci.* **34**, 125 (1984); F. Boehm and P. Vogel, *Physics of Massive Neutrinos*, 2nd ed. (Cambridge University Press, Cambridge, UK, 1992).
 [11] H. Orihara *et al.*, *Nucl. Phys. A* **577**, 9 (1994).
 [12] H. Akimune *et al.*, *Phys. Lett. B* **394**, 23 (1997); **665**, 424(E) (2008).
 [13] M. Bhattacharya *et al.*, *Phys. Rev. C* **58**, 1247 (1998).
 [14] J. Blachot, *Nucl. Data Sheets* **92**, 455 (2001).
 [15] S. Rakers *et al.*, *Phys. Rev. C* **71**, 054313 (2005).
 [16] M. Ichimura, H. Sakai, and T. Wakasa, *Prog. Part. Nucl. Phys.* **56**, 446 (2006).
 [17] M. A. Moinester, *Can. J. Phys.* **65**, 660 (1987); T. Wakasa *et al.*, *Phys. Rev. C* **55**, 2909 (1997); K. Yako *et al.*, *Phys. Lett. B* **615**, 193 (2005).
 [18] I. Hamamoto and H. Sagawa, *Phys. Rev. C* **62**, 024319 (2000).
 [19] H. Condé *et al.*, *Nucl. Phys. A* **545**, 785 (1992).
 [20] K. Amos, A. Faessler, and V. Rodin, *Phys. Rev. C* **76**, 014604 (2007).
 [21] H. Sakai *et al.*, *Nucl. Instrum. Methods Phys. Res. Sect. A* **320**, 479 (1992).
 [22] T. Wakasa *et al.*, *Nucl. Instrum. Methods Phys. Res. Sect. A* **547**, 569 (2005).

- [23] K. Yako *et al.*, *Nucl. Instrum. Methods Phys. Res. Sect. A* **592**, 88 (2008).
- [24] R. Schaeffer and J. Raynal, Program DW70 (unpublished); J. Raynal, *Nucl. Phys. A* **97**, 572 (1967); J. R. Comfort, Extended version DW81 (unpublished).
- [25] M. A. Franey and W. G. Love, *Phys. Rev. C* **31**, 488 (1985).
- [26] S. Hama, B. C. Clark, E. D. Cooper, H. S. Sherif, and R. L. Mercer, *Phys. Rev. C* **41**, 2737 (1990).
- [27] M. Sasano *et al.*, *Phys. Rev. C* **79**, 024602 (2009).
- [28] M. Sasano *et al.*, *Nucl. Phys. A* **788**, 76c (2007). We note that the $\hat{\sigma}_{GT}$ value of 3.2 used in this reference slightly differs from that used in this work.
- [29] A. Faessler, G. L. Fogli, E. Lisi, V. Rodin, A. M. Rotunno, and F. Šimkovic, *J. Phys. G* **35**, 075104 (2008).
- [30] V. A. Rodin and M. H. Urin, *Phys. At. Nuclei* **66**, 2128 (2003).